Stretch-Activation and Stretch-Inactivation of *Shaker*-IR, a Voltage-Gated K$^+$ Channel

Cicely X. Gu, Peter F. Juranka, and Catherine E. Morris

Department of Medicine, University of Ottawa, Neurosciences, Ottawa Health Research Institute, The Ottawa Hospital, Ottawa, Ontario K1Y 4K9, Canada

ABSTRACT   Mechanosensitive (MS) ion channels are ubiquitous in eukaryotic cell types but baffling because of their contentious physiologies and diverse molecular identities. In some cellular contexts mechanically responsive ion channels are undoubtedly mechanosensory transducers, but it does not follow that all MS channels are mechanotransducers. Here we demonstrate, for an archetypical voltage-gated channel (*Shaker*-IR; inactivation-removed), robust MS channel behavior. In oocyte patches subjected to stretch, *Shaker*-IR exhibits both stretch-activation (SA) and stretch-inactivation (SI). SA is seen when prestretch P_{open} (set by voltage) is low, and SI is seen when it is high. The stretch effects occur in cell-attached and excised patches at both macroscopic and single-channel levels. Were one ignorant of this particular MS channel's identity, one might propose it had been designed as a sophisticated reporter of bilayer tension. Knowing *Shaker*-IR's provenance and biology, however, such a suggestion would be absurd. We argue that the MS responses of *Shaker*-IR reflect not overlooked "mechano-gating" specializations of *Shaker*, but a common property of multiconformation membrane proteins: inherent susceptibility to bilayer tension. The molecular diversity of MS channels indicates that susceptibility to bilayer tension is hard to design out of dynamic membrane proteins. Presumably the cost of being insusceptible to bilayer tension often outweighs the benefits, especially where the in situ milieu of channels can provide mechanoprotection.

INTRODUCTION

Mechanosensitive (MS) ion channels are operationally defined by a particular aspect of their behavior during patch clamp recordings: their P_{open} changes with changing membrane tension. When MS channels were first reported (Guharay and Sachs, 1984) some questioned whether the cation currents were carried by discrete proteins, but K$^+$-selective MS unitary currents (Sigurdson et al., 1987) confirmed that channels can be tension-sensitive. Better yet, K$^+$-selective MS channels of two classes, stretch-activated and stretch-inactivated (SA and SI) were found to coexist in membrane patches (Morris and Sigurdson, 1989), suggesting that membrane tension provided channel-specific gating energy. Initially, therefore, the expectation was that special "mechano-gating" motifs would be uncovered in the various channels whose P_{open} changed substantially with stretch. However, an antithetical view of the diversity of MS channels observed by patch clamp is that inherent mechanosusceptibility is widespread among channels because, for stochastic multistate membrane proteins, the likelihood that *all* transition rates are tension-independent is low . . . with the corollary that . . . channels in situ normally rely on cellular mechanoprotection to prevent mechanical interference in gating (cellular mechanoprotection is any long- or short-range feature that minimizes tension changes felt by a channel, e.g., excess bilayer, membrane skeleton, auxiliary subunits).

If this view is valid, then relaxation of mechanoprotection could allow for mechanotransducer currents, and pathological disruption of mechanoprotection (say via membrane skeleton abnormalities) could lead to mechano-leak currents in pathologies (e.g., muscular dystrophy, ischemia, physical trauma).

As a test for the notion that inherent mechanosusceptibility can be unrelated to specialized mechano-gating protein motifs, we turned to an intensively studied channel whose nonmechanical physiology is thoroughly established, namely the voltage-gated K$^+$ channel, *Shaker*. The test system was unabashedly nonphysiological because 1) *Shaker*'s native auxiliary β-subunit (Yao and Wu, 1999) was not provided; 2) an N-terminal truncated (inactivation-removed (IR)) version of the channel with a small foreign C-terminal epitope was used; 3) *Shaker*-IR, an arthropod nerve-muscle channel, was expressed in an amphibian oocyte, an environment unlike its native excitable cells; 4) in most experiments, cytoplasm was missing (i.e., excised patches were used); and 5) the plasma membrane was traumatized because patch clamp plus stretch stimuli unavoidably disrupt membrane skeleton (Small and Morris, 1994) and mechanoprotective membrane undulations (Zhang and Hamill, 2000). Lipid rafts (see Martens et al., 2000), too, may disperse in patches.

Except for stretch, these conditions have been extensively used in studying *Shaker* gating. Although pipette aspiration of a gigaohm-sealed membrane is a convenient way to stretch a membrane patch, the absolute tension produced is at best only estimated (Sachs and Morris, 1998). Thus, to ensure the robustness of our findings, we used mechanically varied recording conditions including large and small patches, excised and cell-attached configurations, positive

and negative pipette pressures. Controlling membrane tension from one stimulus to the next is difficult enough in a given patch, but comparing one patch to another is even more challenging. Accordingly, within-patch comparisons are used where possible, and for between-patch comparisons, data are normalized.

We show that *Shaker*-IR is an MS channel. The message is not "this is a trivial artifact." Quite the contrary. If inherent mechanosusceptibility such as *Shaker*'s is widespread among nonmechanotransducer channels, then various means for protecting channels from bilayer tension in native membrane (Zhang and Hamill, 2000; discussed in Morris and Homann, 2001) should also be equally widespread and will need more attention.

METHODS

Stage V-VI *Xenopus* oocytes defolliculated by collagenase treatment were injected with cRNA for *Shaker*-IR, that is, with the N-terminal inactivation ball removed ($\Delta 6$–46, see Hoshi et al., 1994). The construct, provided by C. Miller, Brandeis University, had an added C-terminal eight-amino acid epitope. The cDNA used to generate RNA was subcloned into a "Melton expression vector," pSP64TM. Immediately before patching, oocytes were briefly shrunk in a hyperosmolar solution (in mM): 200 potassium aspartate, 20 KCl, 1 $MgCl_2$, 5 EGTA, 10 HEPES pH 7.4) for 3–10 min and manually devitellinized.

Fire-polished pipettes were pulled on a two-stage L/M-3P-A vertical puller (Darmstadt, Germany) using thick-walled borosilicate glass N51A (OD > 1.65 mm, ID 1.15 mm; Garner Glass, Claremont, CA) as described previously (Wan et al., 1999). Changes of pipette pressure were achieved as described previously (Small and Morris, 1994) using two pressure transducers DPM-I (Biotek Instrument, Winooski, VT) arranged in series. Currents were recorded using an Axopatch 200B amplifier and TL1 interface for D/A and A/D conversion (Axon Instruments, Foster City, CA) in conjunction with pClamp 6 software (Axon Instruments). The analog pressure trace was also fed via a gain amplifier into the TL1 interface as described previously (Small and Morris, 1994). A two-electrode voltage clamp (Warner Oocyte Clamp 725C) was used for some tests, as noted. Data were analyzed using pClamp 6, SigmaPlot 5.1 (Jandel Scientific, Corte Madra, CA), and Origin 4.1 (Microcal Software, Northampton, MA).

Patch recordings were made with the following pipette solution (in mM): 140 NaCl, 2 KCl, 6 $MgCl_2$, 5 HEPES, pH 7.2 according to Hoshi et al. (1994), plus ~100 μM $GdCl_3$ (see comments below in this section) except where noted. For excised patches the bath ("cytoplasmic") was 140 KCl, 1 $CaCl_2$, 2 $MgCl_2$, 11 EGTA, 10 HEPES, pH 7.2, whereas for cell-attached and two-microelectrode voltage clamp recordings, the bath was 115 NaCl, 2.5 KCl, 1.8 $CaCl_2$, 1 $MgCl_2$, 10 HEPES, pH 7.2.

Gadolinium solutions are unstable and so were made daily from $GdCl_3 \cdot 6H_2O$ (Aldrich, Milwaukee, WI). For patch clamp work, the salt was weighed and added to 20 ml of pipette solution to give 100 μM $GdCl_3$. Measuring a small quantity of highly hygroscopic salt probably gave substantial day-to-day variation in pipette solution [Gd^{3+}], with further variation developing in the course of seal formation. These variations may contribute to the wide range of apparent $V_{0.5}$ we noted for *Shaker*-IR even in excised patches. For two-microelectrode work, oocyte-to-oocyte variation in bath solution [Gd^{3+}] was not an issue because the solution was made in a large quantity and experiments were done over a short period of time using a single batch of solution.

Because our protocols required knowing the foot of $G(V)$, voltage steps were applied to each patch to determine this region. Ideally, the position of $G(V)$ on the voltage axis the should be characteristic from patch to patch, but in practice it was remarkably variable, presumably due to pipette-to-pipette variations in [Gd^{3+}]. Oocyte-to-oocyte variations in the surface chemistry of the plasma membrane (and hence variable charge shielding by Gd^{3+}) may also have been a factor.

Gigaohm seals (to yield cell-attached patches) were made as previously described (Vandorpe et al., 1994) and excised patches were formed by quickly pulling away from the oocyte once a seal had been achieved. For cell-attached patches, the assumed V_{rest} was -50 mV; to indicate that membrane voltages for cell-attached patches are approximate, they are preceded by "~" in the Results.

Membrane tension in patches was increased as previously described (Wan et al., 1999) using negative (suction) or positive (blowing) pressure. The pipettes (2–4 MΩ) and pressures (usually <40 mmHg) were well within the usual range for studying MS channels (Sachs and Morris, 1998); because the membrane tension generated by a given pressure varies between patches, direct comparisons and dose-responses were made using within-patch data. As we were principally monitoring for the occurrence (or not) of mechanoresponses, not quantifying sensitivity changes as we did for native SA channels in situ (Small and Morris, 1994), patch sealing/mechanostimulation history was not tracked.

RESULTS

Shaker-IR in the presence of Gd^{3+}

Voltage steps that elicited small leak and capacitative currents in patches from uninjected oocytes (Fig 1 *a*) elicited typical I_{Sh} currents (Hoshi et al., 1994) in *Shaker*-IR cRNA-injected oocytes (Fig. 1 *b*). I_{Sh} was outward and noninactivating for hundreds of milliseconds and showed voltage-dependent activation and kinetics (S-shaped activation time course) (Fig. 1 *b*). With long, large depolarizing pulses (2 s or more; not shown) slow "C-type" inactivation (Hoshi et al., 1991) became evident.

Gadolinium (Gd^{3+}) used at ~100 μM fully blocked the endogenous MS nonselective cation channels (Yang and Sachs, 1989). Although Gd^{3+} does not abolish TREK-type SA K^+ channel currents (Small and Morris, 1995), it has diverse actions, so 100 μM Gd^{3+} effects on I_{Sh} were characterized by two-microelectrode clamp. Steady-state I_{Sh} (V_m) with or without 100 μM Gd^{3+} data were used to obtain $G(V)$ curves (Fig. 1 *c*), which were fit to a Boltzmann equation, then normalized (Fig. 1 *d*) to the fitted G_{max}. Gd^{3+} significantly decreased G_{max} to $62 \pm 9\%$ ($n = 9$ oocytes, $p < 0.01$, paired *t*-test). G_{max} recovered completely (e.g., Fig. 1, *c* and *d*) upon Gd^{3+} washout. Gd^{3+} also significantly and reversibly shifted half-activation by $+22 \pm 3$ mV (from -19 to $+3$ mV) and decreased the slope factor by 6 ± 2 mV (from 14 to 20 mV) ($n = 9$; $p < 0.01$, paired *t*-tests) without fundamentally altering the sigmoid voltage-dependence of the channels (e.g., Fig. 1 *d*).

Comparable trivalent lanthanide effects are reported for mammalian Kv1.1 expressed in *Xenopus* oocytes (Tytgat and Daenens, 1997) and Gd^{3+} inhibits voltage-dependent Na^+ and K^+ currents in *Xenopus laevis* axons (Elinder and Århem, 1994). For the axonal K^+ current, 60 and 200 μM Gd^{3+} cause 18 and 26 mV rightward shifts, respectively, comparable to our 22 mV shift with 100 μM Gd^{3+} for *Shaker*-IR.
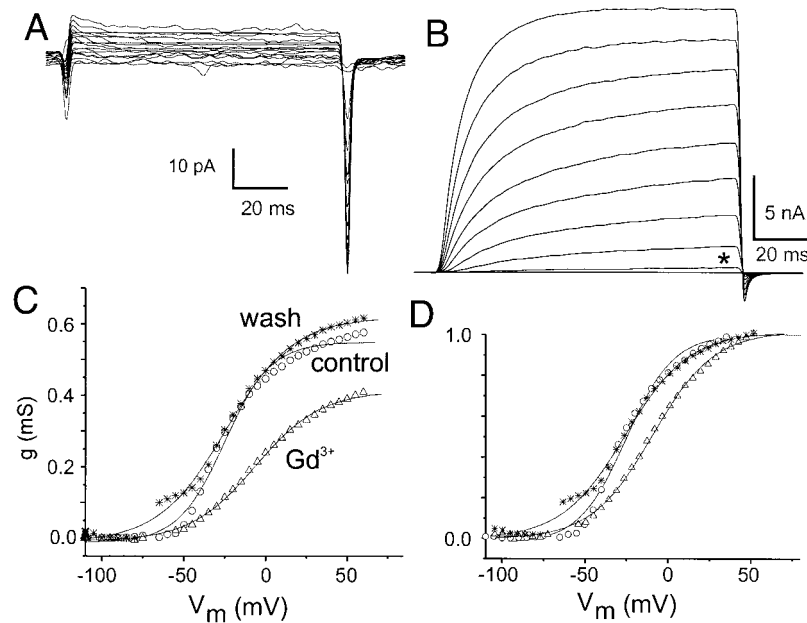
FIGURE 1 *Shaker*-IR currents (I_{Sh}) in *Xenopus* oocytes and effects of Gd^{3+} on I_{Sh}. Currents elicited by depolarizing steps (-110 to $+70$ mV in 10 mV increments, $V_{hold} = -100$ mV, 1 s between successive steps) from inside-out excised patches of (*a*) control (uninjected), and (*b*) *Shaker*-IR cRNA-injected oocytes (asterisk below a 0 mV current trace). Electronic compensation was used to minimize initial capacitative transients. (*c*) Conductance-voltage ($G(V)$) curves from two-microelectrode voltage clamp for a *Shaker*-IR injected oocyte with control (○), 100 μM Gd^{3+} ($\triangle$), and wash-control (∗) solutions perfused into the bath. (*d*) Normalized version of *c*. The solid lines are fits to a Boltzmann equation.

Endogenous MS channels

Because of the worry that residual MS current through endogenous SA cation channels might contaminate *Shaker*-IR records during stretch, we briefly note, for the solutions and recording/stimulating pipettes used in *Shaker*-IR studies, the characteristics of the endogenous SA channels *in the absence of* Gd^{3+} and with no *Shaker*-IR expressed. Pressures of -5 to -30 mmHg activated the channels (the larger the patch, the smaller the pressure required), reversal was near 0 mV, and single-channel conductance was ~ 30 pS at V_{rest} (~ -50 mV). Oocyte patches held at or below V_{rest} exhibited low-frequency spontaneous unitary inward current events (flickery bursts seldom exceeding 10 ms) whose frequency increased reversibly (Fig. 2 *a*) with suction. This sustained P_{open} (open probability) change during high membrane tension represents "classical" MS channel behavior. When both negative (suction) and positive (blowing) pressures were applied to the same patch, each activated the endogenous SA channels (blowing tends to break seals, so suction was routinely used). We did not use "gentle patches" and accordingly did not observe adaptation (Hamill and McBride, 1997).

For all oocyte batches used for *Shaker*-IR data, cell-attached or excised patches from control oocytes were tested with 100 μM Gd^{3+} in the pipette, using a range of voltages and suction pressures. Neither spontaneous nor suction-induced ionic current events were observed ($n > 20$).

Stretch and *Shaker*-IR

Shaker-IR patches were stretched with 100 μM Gd^{3+} in the pipette and I_{Sh} ($= iNP_{open}$, where $i =$ unitary current, $N =$ number of channels in the patch) was recorded. Initially we had *not* predicted that stretch would affect I_{Sh}. Rather, we had made *Shaker*-ankyrin fusion constructs to study spectrin-channel-tension interactions (to test the Guharay-Sachs model of MS channels; Gu et al., 1997). *Shaker* was merely the control. Open and closed conformations are, by definition, equally unstable at the midpoint of the $G(V)$ curve. Our preliminary trials were geared to midregion voltages so that either SI (reduced iNP_{open}) or SA (increased iNP_{open}) effects on I_{Sh} would be evident. The outcome was puzzling. Stretch was not benign, but it had no consistent effect; some patches showed increased steady-state I_{Sh}, some showed a decrease, and some showed increased low-frequency I_{Sh} noise with no change in mean current.

Near the foot of $G(V)$, however, with *Shaker*-IR channels mostly closed yet somewhat destabilized—i.e., exhibiting a detectably non-zero P_{open}—a different story emerged. There, stretch consistently elicited responses like classical SA channels, as in Fig. 2 *b*. We should mention that, having set gains for the mid-$G(V)$ region, we nearly overlooked such responses. Unitary *Shaker*-IR currents are poorly resolved because sampling frequency was for macroscopic I_{Sh}, but outward events are evident. Prestretch P_{open} was low (<0.001 based on the $G(V)$ relation and unitary conductance), but with stretch, NP_{open} reversibly increased ~ 20-
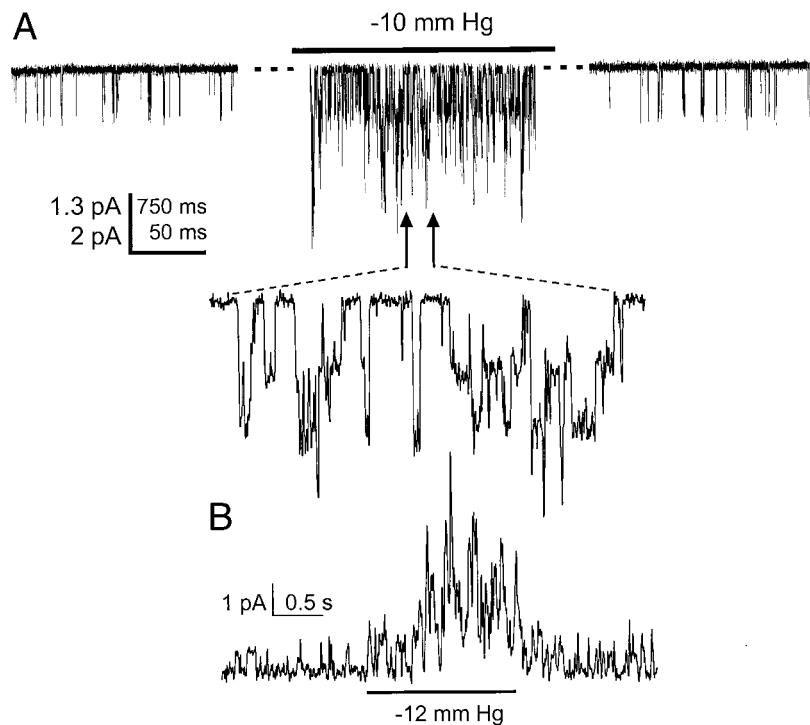
FIGURE 2   Endogenous SA cation channel events and SA events from a *Shaker*-IR-injected oocyte. (*a*) Single-channel recording of endogenous MS cation channel events from a control oocyte (cell-attached patch; no Gd^{3+}; $V_m = \sim -50$ mV) before, during (including expanded section), and after the indicated pipette suction. (*b*) Cell-attached patch-clamp recording ($V_m = \sim -20$ mV) from *Shaker*-IR-injected oocyte in the presence of Gd^{3+}, showing steady-state outward unitary current events, then sustained (and reversible) stretch-activation during pipette suction.

fold. Because endogenous SA currents were blocked and could not in any case have carried outward current at -20 mV, the SA events were attributed to the recombinant *Shaker*-IR channels. *Shaker*-IR-injected oocytes showed SA outward currents near the $G(V)$ foot in all patches tested under similar conditions ($n = 18$).

Stretch at the foot of the *Shaker*-IR $G(V)$

We therefore reexamined stretch effects at the foot of $G(V)$, using voltage-step-plus-stretch protocols to get around a drawback evident in Fig. 2 *b*, namely the lack of the *Shaker*-IR kinetic signature. Generating full current families before, during, and after suction needed at least 2 min per family, during which time rupture was likely. Instead, a truncated approach involving a pair of voltages ("step pair") was used. Patch-to-patch variations in the position of $G(V)$ associated with using Gd $^{3+}$ (see Methods) were dealt with by locating the foot region of $G(V)$ before applying the step pair protocol. A pressure in the range -5 to -20 mmHg was chosen, aiming for a substantial but nonlytic membrane tension (there is an "art" to this; pipette tip size, sealing behavior, and membrane capacitance are the main gauges). The duration of stretch was <10 s. $V_{command}$ for a step pair protocol near the foot of $G(V)$ is illustrated in Fig. 3 (*top right*). The step 1 voltage (duration 150 ms) was chosen to

minimally activate I_{Sh} (usually -20 mV, more rarely -10 mV or 0 mV, depending on $G(V)$ for the patch) and step 2 (also 150 ms) was 10 mV more depolarized. V_{hold} between step pairs was -100 mV. Step pairs were repeated six times (1 s between pairs) before, during, and after stretch to test for repeatability and/or time-dependent trends.

Current traces for this protocol were similar for excised and cell-attached patches. In control patches ($n = 15$) (Fig. 3 *a*) the step pairs elicited small leak currents and capacitative transients. As expected, the second capacitative transient (upward deflection) of the step pair, associated with the 10-mV step, was smaller than the first and third (upward and downward deflections, respectively). Neither leak nor capacitative currents, inspected at high resolution, changed with suction. This indicates a fixed membrane area. Control patch and *Shaker*-IR patch runs were interspersed, with at least one control per batch of oocytes. Occasional tests with suction that would rupture most excised patches (>40 mmHg) showed that even this did not detectably alter capacitative or leak currents. The controls indicated a) no interference from endogenous SA channels and b) suction stimuli did not enlarge the membrane area in the patch.

With *Shaker*-IR patches (e.g., Fig. 3, *b–d*), the step pairs elicited outward I_{Sh} (at step 1, I_{leak} was often distinguishable from I_{Sh}). Currents elicited by the step pair corresponded to "family members" below the asterisk in the full family of
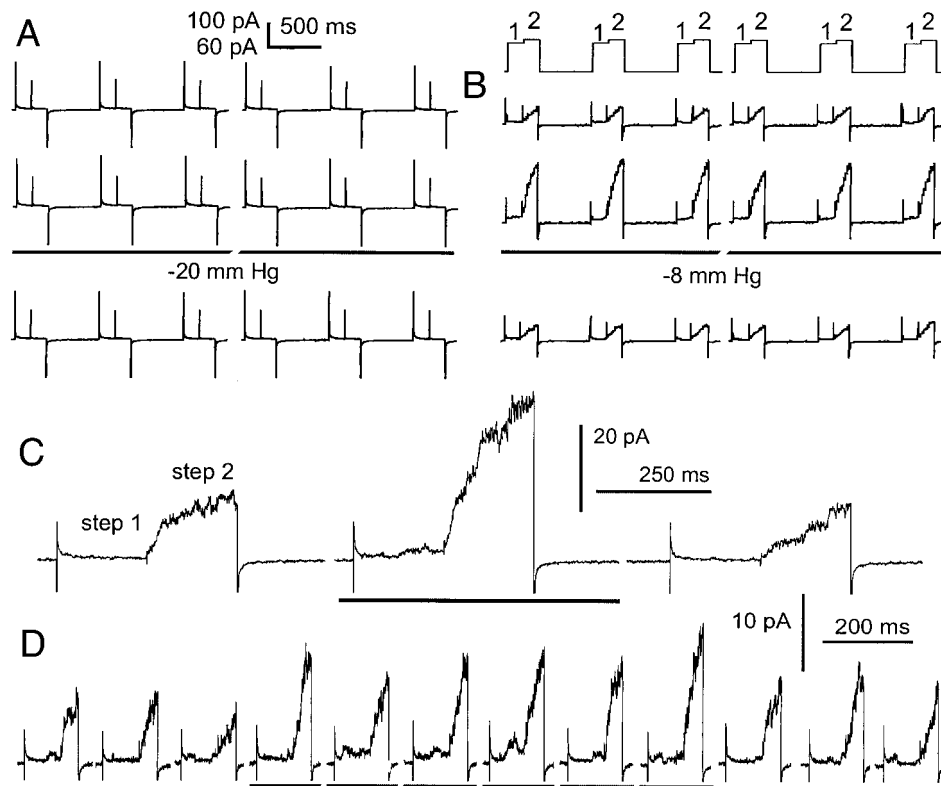
FIGURE 3 Examining SA of *Shaker*-IR by step pair experiments. The top right "battlement" pattern (6 step pairs labeled 1, 2) shows the $V_{command}$ used to elicit the currents illustrated for excised patches of (*a*) one control and (*b*)–(*d*) three *Shaker*-IR-injected oocytes. Pipette solutions had 100 μM Gd^{3+}. V_{hold} was -100 mV and steps 1, 2 were 10 mV apart, as described in the text. Capacitance was compensated before an experiment, then not altered. The protocol was run before, during, and after membrane tension was elevated by pipette suction (*solid bar*); pipette suction in mmHg is indicated for (*a*) and (*b*). In (*a*) and (*b*) gaps correspond to ~1 s, during which the data buffer was emptied and the next run initiated (V_{hold} and pressure were maintained); 100 pA and 60 pA correspond to (*a*) and (*b*), respectively. (*c*) and (*d*) are higher-resolution recordings (unitary events are evident in (*d*)) illustrating I_{Sh} elicited by step pairs before, during, and after stretch (*bars:* -15 and -20 mmHg in *c* and *d*, respectively); one of the six pairs is illustrated per condition for *c*, several in *d* (illustrating large stochastic variation at low NP_{open}). In *c* and *d* most of the current at V_{hold} is omitted (hence the gaps).

Fig. 1 *b* with I_{Sh} showing recognizable activation kinetics most clearly at step 2. With stretch, step 1 and 2 currents increased reproducibly and reversibly ($n = 22$ patches) (Fig. 3 *b*). No time-dependent trends were noted over the six repeats (e.g., Fig. 3, *b* and *d*). In most cases ($n = 15$) the procedure was repeated with the step pair shifted by 5 or 10 mV and again, stretch-augmented I_{Sh} was evident.

These step pair data were quantified as in Fig. 4. For each patch, mean currents ($n = 6$, $\pm$SD) before (0 mmHg, i.e., "control"), during ("stretch") and after ("release") suction were determined (steady-state I_{Sh} or, if current was still rising at 150 ms, maximal I_{Sh}, or, if unitary currents were obtained, time-averaged I_{Sh}). Fig. 4 *a* illustrates a patch whose below-average response allows for display of step 1 and step 2 data on a common *y* axis. For between-patch comparisons, within-patch data were normalized (Fig. 4 *b*) as this partially deals with differences in channel density, patch size, and tension. Between-patch comparisons over the whole data set can be summarized thus: for 17 of 17 patches tested using the step pair -20 mV, -10 mV, suction ($\leq$20 mmHg) increased I_{Sh} at both voltages (paired

t-tests, $p < 0.01$). The fold-increase of I_{Sh} ($I_{test}/I_{control}$) was significantly greater for step 1 than step 2 (3.8 $\pm$ 0.4 for step 1 and 2.6 $\pm$ 0.3 for step 2 (mean $\pm$ SE, $n = 17$, $p < 0.01$)). Thus, in all patches, stretch was disproportionately more effective near the foot of $G(V)$ than 10 mV more depolarized. Fig. 4 *c* plots the outcome for all 17 patches, with the stretch-current (not the control) as unity, thereby emphasizing that I_{Sh} was an "SA channel" over this voltage range.

Higher pressures applied at the end of these experiments consistently elicited larger I_{Sh} increases, indicative of a dose-dependent effect of stretch. Fig. 5 shows dose-dependence for an excised patch subjected to a broad range of pressures. Current amplitudes (Fig. 5 *a*) increased with pressure until patch rupture occurred just after -40 mmHg. Fig. 5 *b* plots fold changes. Patches from three oocytes withstood this treatment, each showing that when the pre-stretch $P_{open}(V)$ values were low but detectably > 0 (i.e., near the foot of $G(V)$), stretch increased iNP_{open} in a dose-dependent manner. In Fig. 5, for step 1, the smallest stimulus (-5 mmHg) almost doubled I_{Sh} and the largest (-40 mmHg) elicited a >10-fold increase. As with the 17 patches
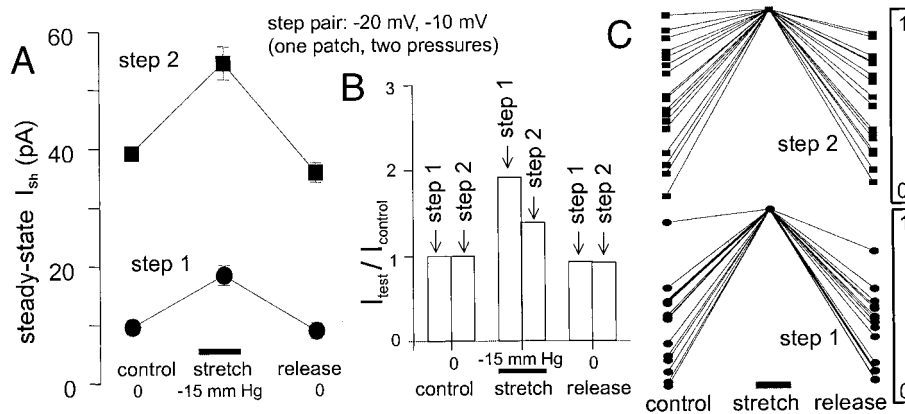
FIGURE 4 Voltage-tension interactions; analysis of step pair data. (*a*) From a sample patch (different patch, but raw data as illustrated in Fig. 3, *b--d*), steady-state I_{Sh} (mean $\pm$ SD, $n = 6$) elicited by step 1 and by step 2 for pipette pressures 0 and -15 mmHg, before (control, "0"), during (stretch, "-15 mmHg"), and after (release, "0") mechanical stimulation. $V_{command}$ for steps 1 and 2 was -20 mV and -10 mV, respectively. Here and elsewhere, steady-state I_{Sh} was obtained by cursor measurement (Clampfit from Axon Instruments' p-Clamp). The baseline was reset to the leak current level where this was evident. (*b*) Mean test I_{Sh} (same data as (*a*)) replotted as ratio of the control I_{Sh} for step 1 and step 2. (*c*) Among-patches comparisons of the relative extent of stretch-activation in 17 excised patches; here, within-patch values have been normalized by setting the mean "I_{Sh} stretch" in each patch to unity. For all 17 patches, the step pair was -20 mV, -10 mV, and in most patches stretch was elicited by -10 mmHg suction. Paired *t*-tests (step 1 [$I_{stretch}/I_{control}$] versus step 2 [$I_{stretch}/I_{control}$] in each patch) showed that the fold-increase nearer the foot of $G(V)$ exceeded that for 10 mV more depolarized ($p < 0.01$).

above, stretch activation was greater on a percent basis at step 1 than step 2 (Fig. 5 *b*), so over a wide range of tensions, stretch was disproportionately a better I_{Sh} activator near the foot of $G(V)$ than 10 mV more depolarized. For step pair data, error introduced if I_{Sh} failed to reach steady-state during a step would *under*estimate, not overestimate, this disproportion because I_{Sh} activation speeds

up with depolarization. Likewise, error from leak currents would contribute to an underestimate. Stretch's disproportionate effect at lower P_{open} (*V*) values is good evidence that it affected *Shaker*-IR gating. Had stretch increased I_{Sh} not through tension effects on gating (i.e., on P_{open}), but by increasing the quantity of *Shaker*-IR-bearing membrane in the patch (hence increasing *N*), then
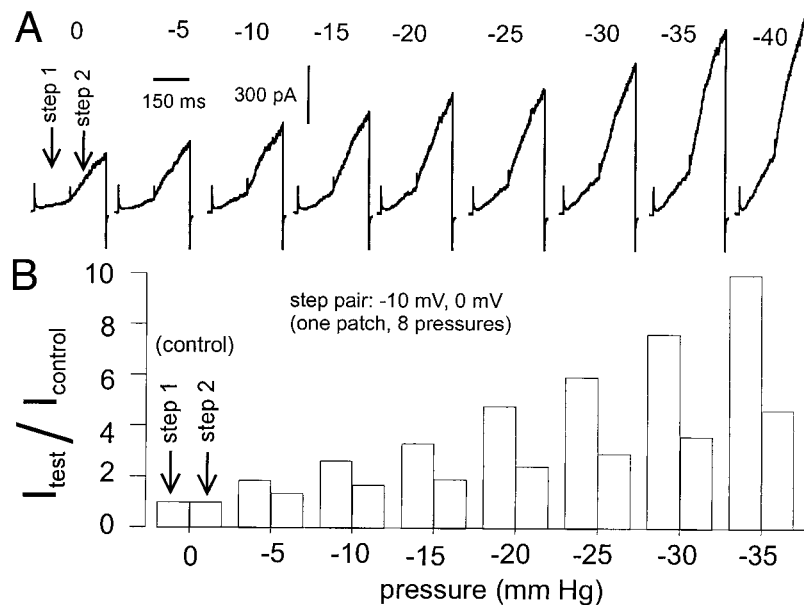

FIGURE 5 Within-patch dose-response over a wide pressure range. (*a*) I_{Sh} traces for a step pair experiment on an excised patch with successively increasing membrane tension (pipette pressure in mmHg is indicated along the top). The step pair voltages (-10 mV, 0 mV) were near the foot of the $G(V)$ for the patch. The step pair was applied once/pressure. (*b*) The currents in (*a*) plotted as a dose-response using the same procedure as in Fig. 4 *b* (except that the step pair was applied only once at each pressure rather than six times). Since step 2 saturated the current amplifier at -40 mmHg, the plot stops at -35 mmHg.

I_{Sh} at the two voltages would have increased proportionately with suction.

Stretch-activation plus stretch-inactivation of I_{Sh}

Preliminary stretch tests at high P_{open} (like Fig. 2 *a*, but for very depolarized voltages) did not yield increases of outward current. Had stretch enhanced nonspecific leak, had it caused "breakthrough" SA cation channel currents, or had it generated additional current through *Shaker* channels, outward current would have resulted. Instead, the effects of stretch at large depolarization looked like a decrease (SI) in I_{Sh}. We therefore examined stretch on I_{Sh} at both extremes of prestretch P_{open} (*V*), using a step protocol so that both voltages extremes were tested during a given mechanical stimulus. For the three patches that withstood a wide range of pressures, effects of stretch near the foot and head of *G*(*V*) are shown in Fig. 6. Steps 1 and 2 (60 mV apart) were chosen after locating *G*(*V*) for the patch. Fig. 6 *a* illustrates current traces (patch 1) at two test pressures. To reduce the possibility of patch rupture, step pairs were applied once (not six times). Suction was held constant for 2 s at each level, the step pair was applied, pressure was increased, and so on. For each patch, where the high prestretch P_{open}(*V*) plots (step 2 for each patch) show a dose-dependent SI trend (I_{Sh} decreasing as pressure increases), simultaneously the low prestretch P_{open}(*V*) plots show a dose-dependent SA of I_{Sh}. In other words, in immediately adjacent 150-ms periods (with the stretch stimulus unchanged), the population of *Shaker*-IR channels in any given patch exhibited dose-dependent SA and SI.

Possible sources of artifacts

Mechanical stimulation of soft biomaterial is unavoidably messy. Although patch aspiration is the best method for transiently increasing plasma membrane tension, it is a poorly controlled stimulus, making it imperative to probe the robustness of stretch effects. One concern is that after gigaohm seal formation residual pressure of unknown value may persist (Morris and Sigurdson, 1989). If so, application of a small pressure step (say, in the ±1–10 mmHg range) might either increase or decrease the net pressure by opposing the residual value. Accordingly, it was reassuring that the dual outcomes of Fig. 6 (i.e., SA-plus-SI) were observed over a large pressure range. Furthermore, for negative pressures that would have far exceeded any inadvertent positive pressure, exactly the same suction stimuli that augmented I_{Sh} at one voltage (step 1) diminished it at another (step 2). This essentially eliminates the possibility that stretch effects on I_{Sh} resulted from transient membrane area increases.
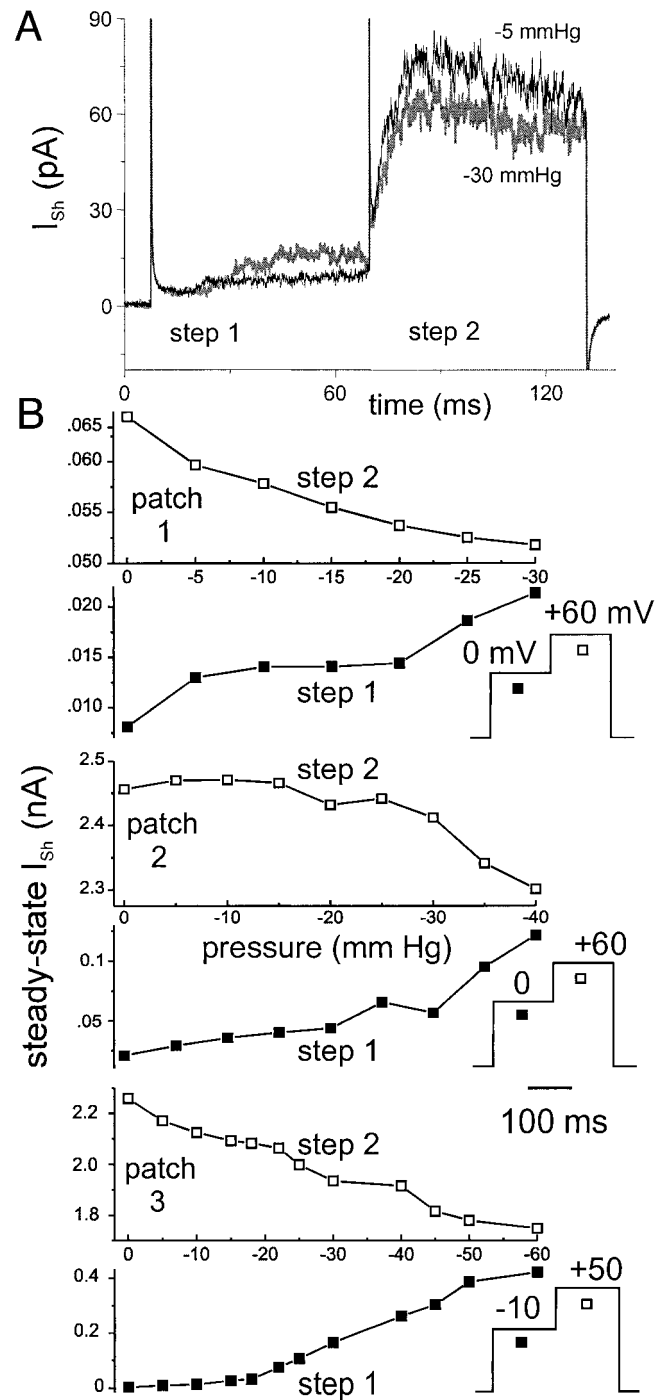

FIGURE 6 Within-patch pressure dose-responses for "foot-to-head" step pairs. (*a*) Raw step pair currents from patch 1 (see (*b*)) at two different test pressures. (*b*) Steady-state I_{Sh} from three excised patches using 60-mV step pairs at the indicated voltages. I_{Sh} magnitudes differed greatly 60 mV apart and so are plotted separately with different *y* axis gains. The particular step pair for each patch is indicated (■, step 1; □, step 2).

It was also crucial to establish that stretch effects ascribed to *Shaker*-IR were not in fact "contamination currents" from inadequately blocked endogenous SA cation channels. Two measures to rule this out have been mentioned: noninjected

oocytes were examined and SA of *Shaker*-IR was studied near V_{rev} of the endogenous SA channels. A third approach is a direct demonstration that even without Gd^{3+} (or with "break-through" of the Gd^{3+} block), endogenous SA currents would not explain effects seen in *Shaker*-IR patches. Fig. 7 *a* shows the endogenous SA cation currents (control oocyte, no Gd^{3+}) reversing near 0 mV. As is common, a secondary mechanical effect is evident (baseline SA channel activity did not return immediately to the prestretch level). The next traces (Fig. 7, *b* and *c*) are for *Shaker*-IR-injected oocytes over a voltage range. Steady-state voltage-gated I_{Sh} was established by stepping (not shown) from −100 mV to a depolarized voltage for 10 s, during which time suction was applied twice. In Fig. 7 *b*, suction increased the steady-state current at the least depolarized voltage (∼−30 mV), produced an equivocal increase at a voltage 10 mV more depolarized, then reproducibly decreased the current 20 mV beyond that. Unequivocal stretch-induced changes were associated with the voltage "extremes" (foot and head of $G(V)$) rather than the intermediate voltages (e.g., +20 mV in Fig. 7 *c*). At intermediate voltages, SA and SI effects on current were presumably sufficiently balanced across the population of channels that they tended to cancel.

Currents through inadequately blocked endogenous MS channels could not have produced the stretch-induced pattern of changes in Fig. 7, *b* and *c*. Voltage-dependent I_{Sh} was exclusively outward at all test voltages, whereas the endogenous SA channel exhibited inward currents when $V_m < V_{rev}$ and outward currents when $V_m > V_{rev}$ (Fig. 7 *a*). Given their particular V_{rev} values (∼0 mV versus ∼−80 mV), combining endogenous SA currents with steady-state $I_{Sh}(V)$ would have produced a strong (mis)impression of SI of I_{Sh} at hyperpolarized potentials and of SA of I_{Sh} at depolarized potentials. Precisely the opposite was observed (Fig. 7, *b* and *c*).

For ENaC channels reconstituted into bilayers, release from calcium block during application of hydrostatic pressure was misconstrued as MS gating (Ismailov et al., 1997). For *Shaker*-IR in oocytes patches, SA and SI of I_{Sh} occurred in the absence of Gd^{3+} and therefore were not release-from-block effects. A trace showing SI of I_{Sh} in a *Shaker*-IR patch in the absence of Gd^{3+} (Fig. 7 *d*) illustrates this point. The endogenous SA channels probably added a component of MS outward current during the two stretch stimuli, but obviously this would not explain a net *decrease* in outward current during stretch. Although we cannot rule out that stretch/Gd^{3+} interactions at the mem-
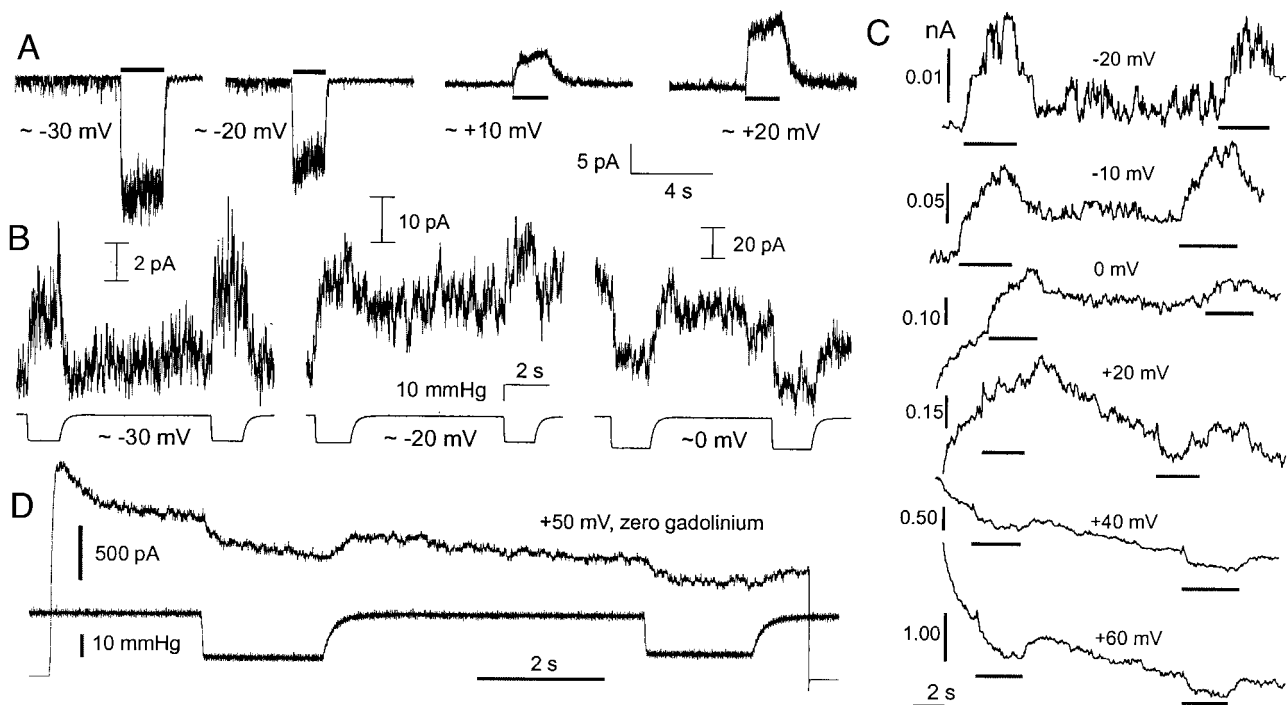

FIGURE 7 Suction effects on I_{Sh} and endogenous SA currents. (*a*) Endogenous SA I_{cation} elicited by suction of −20 mmHg (*bars*); cell-attached patch, noninjected oocyte, V_m as indicated, no Gd^{3+}. (*b*) Cell-attached patch clamp trace, Gd^{3+} in the pipette, *Shaker*-IR injected oocyte. Pipette pressure traces are below the current traces; downward deflection indicates negative pressure (suction), V_m as indicated. In the last current trace, slow (C-type) inactivation of I_{Sh} is evident. Note each current trace has its own scale. (*c*) Excised patch clamp trace, Gd^{3+} in the pipette, *Shaker*-IR-injected oocyte, suction (−15 mmHg) applied as indicated by bars. Again, each trace has its own scale. Pronounced C-type inactivation of I_{Sh} is evident in the last two traces. (*d*) Excised patch, with zero Gd^{3+} in the pipette, *Shaker*-IR-injected oocyte (traces as in (*b*), except that current is shown at −100 mV, then +50 mV, then −100 mV, and the pressure and current traces overlap).

brane modified the responses of *Shaker*-IR to stretch, Gd^{3+} did not cause them.

Tension versus membrane curvature

To determine whether membrane tension was the relevant mechanical stimulus during SA and SI of I_{Sh}, excised patches at a fixed voltage were subjected to suction, then blowing. Fig. 8 shows that suction and blowing elicited qualitatively the same response. Where suction increased I_{Sh} so did blowing, and where suction decreased I_{Sh} so did blowing. Thus, tension, independent of the sign of membrane curvature, was the critical mechanical stimulus. The other option—that both suction and blowing increased I_{Sh} by reversibly augmenting membrane area in one voltage range while, in another range, both suction and blowing decreased I_{Sh} by reversibly diminishing membrane area—is wholly implausible.

Stretch-activation I_{Sh} at the single-channel level

Finally, effects of tension on *Shaker*-IR were examined at the single-channel level, typically using patches smaller than for macroscopic I_{Sh}. A greater fraction of channels/patch responded to stretch in single-channel studies than in the macroscopic current studies. It was harder forming seals with the smaller patches needed for single-channel recording, so these patches were probably quite traumatized. Because membrane trauma renders various channels more, not less, susceptible to stretch (TREK-type channels, Small and Morris, 1994; Wan et al., 1999; NMDA channels, Paoletti and Ascher, 1994; Na^+-channel α-subunits, Tabarean et al., 1999) it may have enhanced "recruitment" by stretch in the

FIGURE 8 Suction and blowing have equivalent effects. I_{Sh} in two excised patches (*a* and *b*),V_m as indicated, and patch tension generated using both concave patch (suction) and convex patch (blowing) configurations. The pressure traces are shown below each current trace. C-type inactivation is evident in (*b*).

single-channel studies. Applied to patches, Laplace's law dictates that the smaller the patch radius of curvature, the greater the pressure required for a given tension, hence the larger pressures used in this section.

Bearing in mind the $G(V)$-shifting and G-decreasing effects of Gd^{3+} on I_{Sh} (Fig. 1 *c*), single-channel characteristics at resting membrane tension were as expected for *Shaker*-IR (Hoshi et al., 1994). Because patches had multiple channels, unitary events were best resolved at membrane potentials and/or tensions that yielded small P_{open} values. Fig. 9 *a* illustrates single-channel data from an excised patch with a low prestretch P_{open}. Increasing stretch intensity (pressures 0 to -20 mmHg) increased NP_{open}, presumably via P_{open}. The effect was reversible upon release (see bottom trace, 0 mmHg). The pressure-family of current amplitude histograms (Fig. 9 *b*) indicates that stretch-sensitive current was associated with *Shaker*-IR, not, say, breakdown noise; equal intervals of $\sim$0.6 pA between baseline and the subsequent amplitude peaks indicate that the same class of channel contributed at low, intermediate, and high current levels. This also confirms that membrane stretch did not increase *Shaker*-IR iNP_{open} by changing i, the unitary current amplitude (as might occur if, say, stretch reduced the *Shaker*-Gd^{3+} interaction that diminishes G_{Sh}).

Single-channel dose-responses for this and five other patches (Fig. 9 *c*) were fit to sigmoids that have been normalized for display purposes. Each dose-response has a steeply rising activity (pressure) region, typical of most SA channels. The total number of stretch-responsive *Shaker*-IR channels in the patch was unknown because all patches ruptured before showing convincing saturation (patches ruptured after the highest pressure for which data are given). We therefore have not extracted Boltzmann parameters (slope factor and half-maximum P_{open}) from the curves.

Wide variability in the location of SA curves along the pressure axis, as in Fig. 9 *c*, is typical for SA channels (Gustin et al., 1988; Sachs and Morris, 1998; Vandorpe et al., 1994) because tension (dependent on the membrane's radius of curvature) is the operative *x* axis variable, not applied pressure. Probably the three leftmost curves represent larger patches with larger radii of curvature.

For one of the six patches (*inset*, Fig. 9 *c*), both positive and negative pressures were applied. For this excised patch, P_{open} at 0 mmHg was marginally above zero. As mentioned for macroscopic I_{Sh}, pressure at both signs, "blowing and suction," should elevate membrane tension, with membrane curvature directed out of or into the pipette tip, respectively. The resulting SA dose-response, a classical U-shape, confirms at the single-channel level that increased membrane tension underlies I_{Sh} responses to changes in pipette pressure.
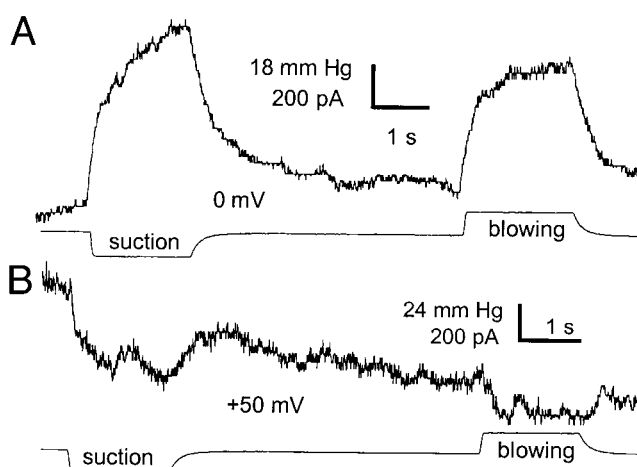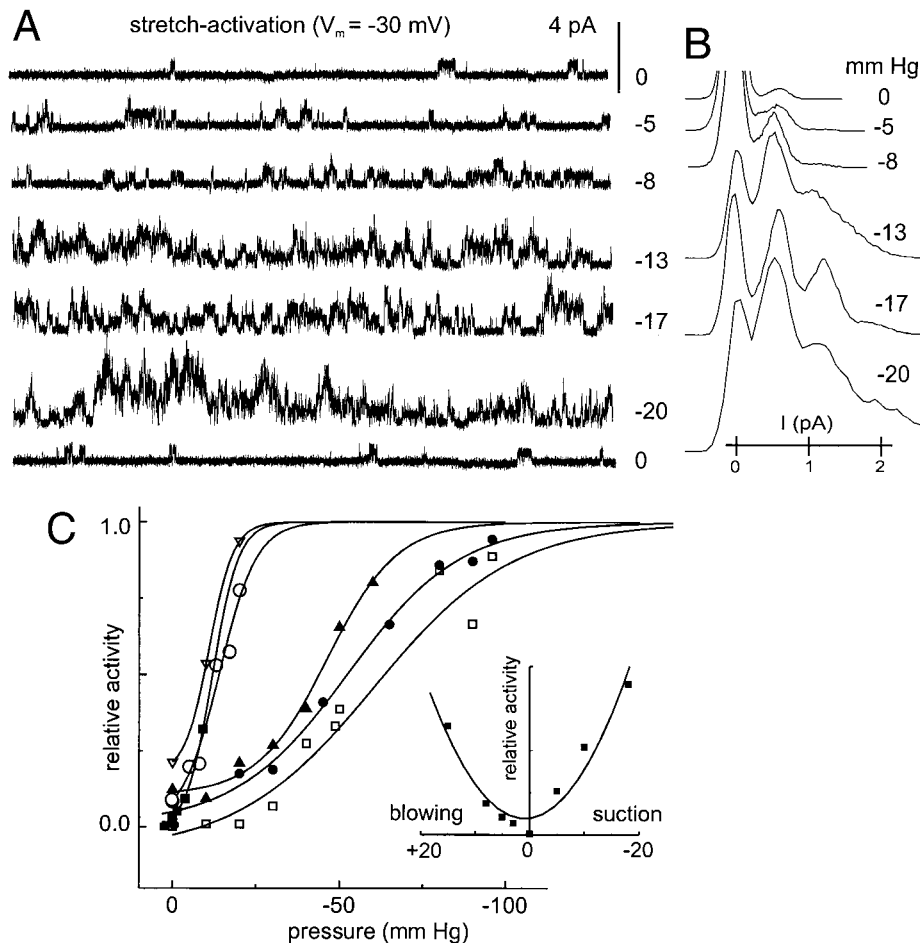
FIGURE 9 Effect of increasing suction on single I_{Sh} and on the P_{open} of *Shaker*-IR. (*a*) Five-second current trace excerpts, excised patch, pipette pressure in mmHg as indicated. Each pressure was applied for 20 s, then switched to the next level. The last trace was after suction was released to 0 mmHg from -20 mmHg. $V_m = -30$ mV. (*b*) All-points current amplitude histograms for the same data set as in (*a*) (and same as *open circles*, (*c*)). On the current amplitude axis, "0 pA" (no open channels) is the mean of the Gaussian baseline current (peak truncated in some cases). (*c*) Dose-response data as in (*a*) for six excised patches. Each point represents an average NP_{open} computed from a continuous 20-s recording. V_m values were -30 mV ($\triangledown$); -30 mV ($\blacksquare$); -20 mV ($\bigcirc$); -10 mV ($\blacktriangle$); 0 mV ($\bullet$); and 5 mV($\square$). Pressure was increased progressively without release between successive pressures, except for one patch ($\square$), which was done in reverse order. *Inset:* a U-shaped dose-response resulted when patch $\blacksquare$, whose activity was low but non-zero at 0 mmHg, was subsequently subjected to a series of positive and negative pressures (the fit is for display purposes and implies no precise function).

Stretch-inactivation of I_{Sh} at the single-channel level

SI of I_{Sh}, too, was evident at the single-channel level, as illustrated (Fig. 10) for an excised patch where suction, applied twice, reversibly "turned-off" most of the voltage-activated *Shaker*-IR channels in the patch. Post-suction recovery was noninstantaneous partly because decay of applied pressure on release of suction was slower than pressure onset (see typical pipette pressure traces in Figs. 7 and 8), but beyond this instrumentation effect, asymmetric responses (faster onset than offset) are common for MS channels (e.g., see Fig. 7 *a*, endogenous channel) including a neuronal SI K^+ channel (Small and Morris, 1994; Fig. 2 *b*). This may relate more to patch mechanics than channel properties per se. Rapid, reversible, reproducible switching

between multiple- and single-channel recording of I_{Sh} as seen in Fig. 10 supports the earlier argument (based on macroscopic data alone, as in Figs. 6–8) that suction-induced SI of I_{Sh} represented a tension-induced decrease in *Shaker*-IR P_{open}.

Single-channel SI I_{Sh} dose-response data are illustrated in Fig. 11 *a* for an excised patch at $+20$ mV and a series of increasingly negative pressures. By -50 mV, stretch completely silenced the voltage-activated events. Next, at 0 mmHg (penultimate trace), the patch was stepped down by 30 mV to -10 mV, i.e., the foot of $G(V)$ for the patch, yielding a low level of channel activity. The pipette pressure was again increased sequentially; a trace at -50 mmHg is illustrated. Here, at the foot of $G(V)$, SA is observed (as in Fig. 9 *a*). Unequivocally, SI and SA of *Shaker*-IR can be
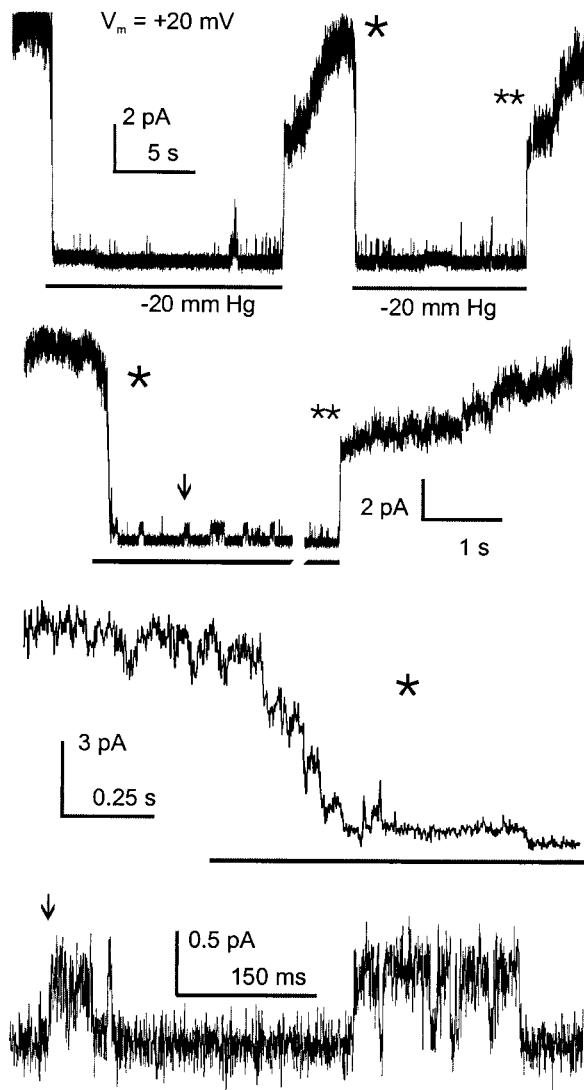
FIGURE 10 Reversible stretch-inactivation of I_{Sh} at high P_{open}. I_{Sh} from a depolarized ($V_m = +20$ mV) excised patch. When suction was applied and released twice, I_{Sh} changed reversibly from a macroscopic (multichannel) to a single-channel trace. Below, this trace is seen at expanded time resolutions, with locaters provided. The trace is interrupted in the second line. Channel activity turned off via discrete current steps (*third line*). Suction is indicated (*bar*) except in the last line, when it was continuous.

elicited from the same patch. If it is striking to compare $+20$ and -10 mV traces for 0 mmHg, it is spectacular to compare them for -50 mmHg; -50 mmHg completely abolished channel activity at $+20$ mV but had the opposite effect at -10 mV, producing intense channel activity from a near-silent patch. Thus, depending on prestretch P_{open}, *Shaker*-IR channels can be either SA channels or SI channels.

As an aside, the 30 mV increase in driving force at $+20$ mV versus -10 mV probably accounts for most of the increase in unitary current, but relief of fast block of the *Shaker*-IR channels by Gd^{3+} at more depolarized potentials may also contribute.

Fig. 11 *b* uses the entire 20-s record traces from the same patch (Fig. 11 *a* shows 5-s excerpts plus two additional 800-ms traces) to plot normalized NP_{open} as a function of pressure, showing that SI of single-channel I_{Sh} was dose-dependent and that SA occurred over the same pressure range. Obtaining SA or SI responses depended on whether channels were mostly quiescent (SA) or mostly active (SI) before stretch, i.e., whether the holding potential was -10 mV (SA) or $+20$ mV (SI). The overlapping dose responses for the two voltages corroborates the macroscopic data (Fig. 6), indicating again that SI and SA can occur in the same patch.

Although Fig. 11, *a* and *b* was the only patch yielding a full single-channel dose response at both low and high prestretch P_{open}, single-channel SI dose responses for several patches held at potentials between $+20$ mV and $+60$ mV are shown in Fig. 11 *c*. For between-patch comparisons, dose (pressure)-dependent channel activity is plotted as normalized NP_{open}. Patch rupture was a problem, though near-zero activity levels were obtained before rupture in three of five patches. Single-channel dose responses (plus the macroscopic ones, Fig. 6) at high prestretch P_{open} showing an inverse relation between *Shaker*-IR NP_{open} and applied suction signify that *Shaker*-IR can be considered an SI channel and an SA channel.

DISCUSSION

Shaker-IR: an MS channel "ordinaire"

The early view (Guharay and Sachs, 1984) that MS channels are specially designed physiological mechanotransducers has been controversial (Morris, 1992; Sachs and Morris, 1998), and except for prokaryote osmotic safety valves—the MscL channels (see Sukharev et al., 2001)—evidence that particular MS channels are mechanotransducers remains threadbare (e.g., Sachs et al., 2000). MscL, strikingly, is designed to be stretch-*in*sensitive until tension becomes near-lytic (Batiza et al., 1999). In contrast, *Shaker*-IR routinely responded to stretch at comfortably nonlytic tensions, as do neuronal SIK channels (Morris and Sigurdson, 1989) and SAK (TREK-type) channels (Wan et al., 1999; Patel et al., 1998) and oocyte SA channels. None are mechanotransducers (e.g., Steffensen et al., 1991; Morris and Horn, 1991; Wilkinson et al., 1998). Its tension/voltage interactions aside, *Shaker*-IR behaved as a "standard" MS channel during patch clamp (macroscopic and unitary patch currents), showing dose-dependent, sustained, reversible responses, with membrane tension the relevant mechanical stimulus, and with stretch able to produce a one-to-two orders of magnitude ΔNP_{open}. Several other voltage-gated channels respond to membrane stretch. Smooth muscle calcium currents increase reversibly with inflation (Langton, 1993). Ca^{2+}-activated large-K^+ channel can be stretch-activated independent of calcium (Lee et al., 2000). The skeletal
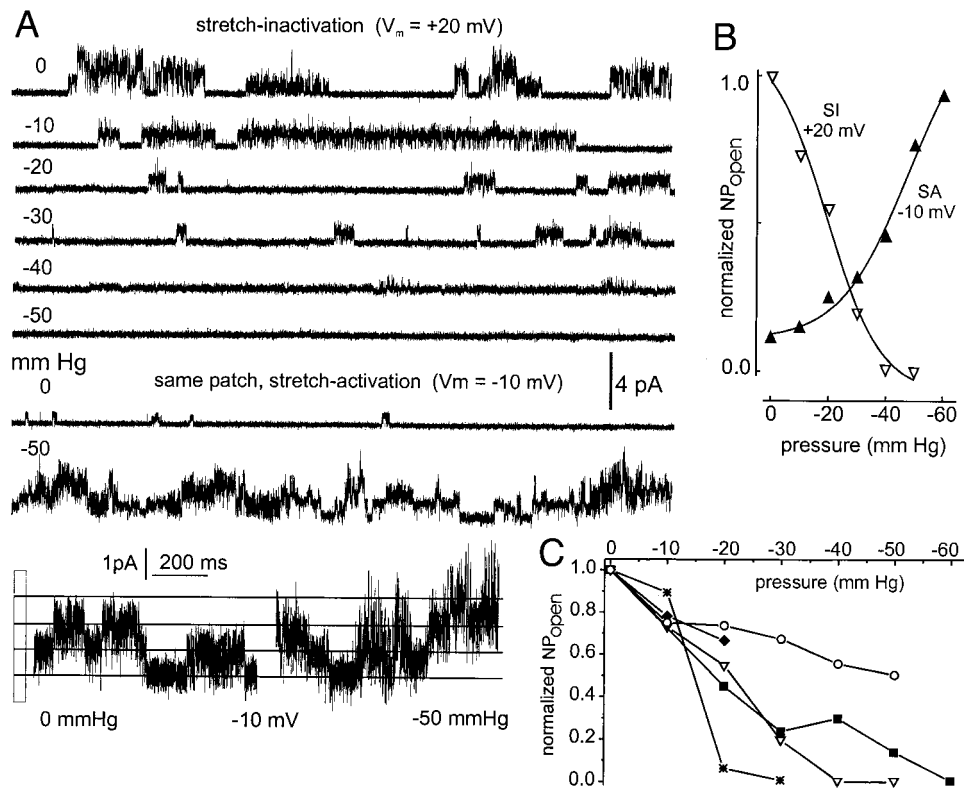
FIGURE 11 High versus low prestretch P_{open} (V_m), single-channel data. (*a*) Five-second current traces from 20-s continuous recordings, collected in the sequence shown. After the series at $V_m = +20$ mV, the patch was clamped at $V_m = -10$ mV and taken from 0 to -60 mmHg in 10 mmHg steps (not all shown). The two higher-resolution fragments of -10 mV current trace (*bottom*) are provided to allow for comparison of current amplitudes during periods of exceptionally high activity at 0 mmHg and of exceptionally frequent transitions at -50 mmHg. (*b*) SA and SI dose-responses for this patch at $V_m = +20$ mV ($\triangledown$) and $V_m = -10$ mV ($\blacktriangle$) using normalized NP_{open}. The fits are for display. (*c*) Single-channel dose-responses (protocol as in Fig. 9, with NP_{open} calculated from 20-s recordings) from five excised patches at depolarized (elevated NP_{open}) voltages: $+60$ mV($*$); $+40$ mV ($\bigcirc$); $+60$ mV ($\blacklozenge$); $+20$ mV($\triangledown$, same as in (*b*)); $+60$ mV ($\blacksquare$). NP_{open} values were normalized for each patch.

muscle Na^+ channel α-subunit, expressed in *Xenopus* oocytes, does not show reversible effects as seen in *Shaker*, but its anomalously slow inactivation irreversibly converts to normal inactivation with stretch (Tabarean et al., 1999). Although *Shaker*-IR's reversible responses to stretch are more akin to those of TREK than the irreversible response of the Na^+ channel, it would seem absurd to invoke sequence similarities or differences to explain any of this.

The biology of mechanosusceptibility

Shaker-IR was mechanosusceptible under profoundly non-physiological conditions. Even minus its cytoplasmic S3-S4 linker (Tabarean et al., 2000), *Shaker*-IR retains mechanosusceptibility. Clearly this is a deeply embedded biophysical trait, but what might it signify in biological, i.e., in evolutionary terms? Here are two opposing evolutionary hypotheses to account for the observation that diverse unrelated channel types, *Shaker*-IR included, are MS channels: 1) MS channels respond to bilayer tension because evolutionary design provides them with specialized mechanogating regions and/or a special global structure that renders

them susceptible to bilayer tension; 2) MS channels respond to bilayer tension because it has been impossible, undesirable, and/or unnecessary to eradicate protein characteristics whose side effect is mechanosusceptibility. The two likeliest "side effects" are a) at least one of the channel's multiple conformations has a different in-plane area than the others; and b) the channel has domains that are deformable by sublytic bilayer tension. Options a and b are not mutually exclusive.

We prefer hypothesis 2 for *Shaker*-IR. Increasingly, the idea that mechanosusceptibility is hard to design *out* of membrane proteins seems more compelling than the idea that mechanosusceptibility is hard to design *in* to membrane proteins. Ironically, the ample selection of MscL mutants that produce a channel *more* mechanosusceptible than the wild type (Batiza et al., 1999) make the same point. If 2a and/or 2b apply, it is easy to suggest why natural selection has failed to eradicate mechanosusceptibility from many nonmechanotransducer ion channels. For 2a, restricting a membrane protein to fixed-area conformation changes would greatly restrict its range of molecular motions. For 2b, pervasive internal cross-linking that rendered a channel

nondeformable would exact a heavy cost in the guise of low frequency of thermal transitions, and hence long response times to significant stimuli.

Conformation area and/or deformability

Shaker-IR behaved as an MS channel in excised oocyte plasma membrane. Although MscL requires only an artificial bilayer for SA gating (Sukharev et al., 2001) the SA-plus-SI behavior of *Shaker*-IR may require a more complex environment. Excised oocyte membrane is a potpourri of diffusible and anchored lipids, transmembrane proteins, and membrane skeleton remnants and, possibly, lipid subdomains. Below we consider one model that invokes plasma membrane heterogeneity and one that does not.

Consider a two-state (C↔O) channel in a Hookean bilayer: if state O occupies more in-plane area, it will be favored by high tension because, under stretch, the channel need do less bilayer-compressing work to expand to O. A "big area O" channel would be an SA channel, whereas a "big area C" channel would be an SI channel (see Sachs and Morris, 1998). *Shaker*-IR exhibits SA and SI behavior, which a two-state area model cannot accommodate, but addition of one additional state (e.g., C↔C↔O or C↔O↔C) should, in principle, and *Shaker*-IR has many kinetically distinguishable kinetic states, mostly closed (Hoshi et al., 1994; Bezanilla, 2000). Unless all occupy precisely the same in-plane membrane area, *Shaker*-IR should exhibit some degree of mechanosusceptibility. Although simultaneous fluorescence/gating charge probes of transitions among *Shaker* closed states strongly suggest that gating motions have vectors in the bilayer plane, the models depicting the moving parts have not, to date (see Fig. 16 in Bezanilla, 2000) specified net area differences. However, it remains to be established whether *Shaker* conformations are indeed size-invariant in the plane of the bilayer.

If *Shaker*-IR deforms uniformly under tension, the deformed channels could have abnormal transition rates, hence SA or SI should result. If instead, bilayer heterogeneity renders a macroscopic membrane tension nonuniform at the level of individual channels, SA-plus-SI behavior might result in the following way: during stretch, two channels could experience different microforces such that one moved to the left (SI) and the other moved to the right (SA) along multistate kinetic schemes like those below. The resulting dual effects would cancel out at some voltages, but not at others. Before elaborating on tension/voltage interactions, however, we note a fundamental difference between Δ-area versus deformation models. A central assumption of the former is that channels have hard discrete-sized states, whereas an assumption of the latter is that channels (or some part of them (Zaccai, 2000)) are soft enough to be reshaped by tensile forces acting in the plane of the bilayer.
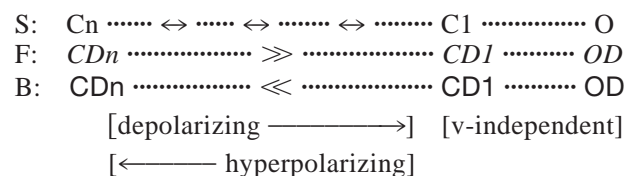
Stretch/voltage interactions in *Shaker*-IR

A simplified kinetic scheme for voltage dependence in *Shaker*-IR is

Cn ······· ↔ ······· ↔ ······· ↔ ·············· C1 ·················· O

[depolarizing ——————→] [v-independent]
[←———— hyperpolarizing]
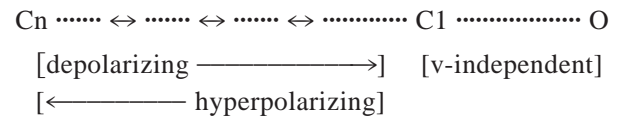
Voltage-dependent transitions taking *Shaker*-IR from Cn to C1 involve rearrangements of the voltage sensor (to a first approximation, the S4s (Bezanilla, 2000)). What if C1 (all S4s repacked) occupies more area than any of the other states? Might that explain our data (i.e., net SA and net SI at slightly depolarized and highly depolarized voltages, respectively)? "Big C1" is probably not the explanation for our observations. If it were, stretch would dramatically increase the duration of within-burst closed events during both SA and SI, and no such effect was seen in single-channel records. Also, we obtained strong SI in cases (e.g., Fig. 11 *a*) that fell well short of the "O dominates" condition. It is possible but not self-evident that *Shaker*-IR has a "big intermediate C" (a C less proximal to O) that produced effects such as we observed. Tests for mechanosusceptibility would be worthwhile for bacterial K_{CSA} (gated by pH rather than voltage), whose transmembrane segments may repack to occupy different areas during gating transitions (Perozo et al., 1998).

Next we sketch a heterogeneous stretch-deformation scheme of *Shaker*-IR that yields SA plus SI. Individual channels in a heterogeneous bilayer deform differently. Channels not appreciably deformed by stretch would maintain their standard (S) transition rates. Stretch-deformed channels showing a net increase in either forward (F) or backward (B) rates would be designated SA or SI, respectively.

S: Cn ······· ↔ ······ ↔ ········ ↔ ········ C1 ················ O
F: *CDn* ···················· ≫ ···················· *CD1* ·········· *OD*
B: CDn ···················· ≪ ···················· CD1 ·········· OD
[depolarizing ——————→] [v-independent]
[←——— hyperpolarizing]

In a patch with 100 *Shaker*-IR channels, let 80, 10, 10 channels be S, F, B, respectively. If prestretch $P_{open} = 0.01$ and if during stretch P_{open} of channels F and B is 0.1 and 0.001, respectively, then I_{Sh} (where i = unitary current, say, 1 pA) is

pre-stretch $iNP_{open} = 1$ pA
                versus
stretch $iNP_{open} = [(80 \times 0.01) + (10 \times 0.1)$
                $+ (10 \times 0.001)] = 1.81 pA$

and this constitutes a net stretch-activation. Now consider stretch-inactivation, i.e., an increased "P_{closed}," where $P_{closed} = 1 - P_{open}$. If V_m is changed so that prestretch

$P_{closed} = 0.01$, comparable channel deformation effects (i.e., 80 unaffected, 10 experiencing 10-fold P_{closed} increase, 10 experiencing 10-fold P_{closed} decrease) will yield a net stretch-inactivation of I_{Sh}. At voltages where pre-stretch $P_{open} = P_{closed} = 0.5$, balanced increases in forward and backward transitions would obscure the microscopic effects of stretch on the steady-state current.

Conti et al. (1984), having analyzed ionic (Na^+, K^+) and gating (Na^+ channel) currents at normal and elevated pressures in squid axon, suggested that a late, rate-limiting activation step not accompanied by easily detected charge movement has a large positive activation volume (volume associated with a reaction's transition state). This could be broadly consistent with a scheme in which voltage-gated channels expand in the plane of the bilayer as they go from C_n to O.

Our underlying assumption has been that what we called stretch-*in*activation is really (i.e., "really" in the parlance of voltage-gating) stretch-*de*activation. That assumption may, however, be unjustified because in addition to its O and C states, *Shaker*-IR can also access (albeit on a time scale of >10 s) inactivated (*I*) states (Bezanilla, 2000). This process is called, in reference to the C-terminus and the pore region, C-type and P-type inactivation. At high P_{open} *Shaker*-IR may, as we have assumed, principally re-enter closed ($C_n - C_1$) states (formally, this would be stretch-*de*activation) but our experiments did not rule out the possibility that, instead, at high P_{open} stretch favors large-area (compared to C_n) C-type and/or P-type inactivated states. In linear schemes, these states would be to the right of and coupled to (Loots and Isacoff, 2000) the "O" state. We note, however, that Meyer and Heinemann (1997) from a thermodynamic analysis of *Shaker*-IR currents measured over a temperature and pressure range, suggest that the C-type inactivated state occupies a smaller volume than the noninactivated state.

Other MS channels that show both SA and SI gating

MS cation channels in healthy muscle exhibit SA, whereas in dystrophic muscle they exhibit SI (Franco-Obregon and Lansman, 1994). For unknown reasons the dystrophic muscle channels have a significantly higher prestretch P_{open} than healthy muscle channels (for *Shaker*, voltage produces such a difference). If the dystrophic situation represents maximal P_{open}, then stretch could produce SI (or have zero effect), but could not produce SA. Given the different membrane skeletons involved (plus or minus dystrophin), channels may experience microstresses that favor high P_{open} in healthy membrane and low P_{open} in dystrophic membrane. In other words, the general factors we invoked for *Shaker*-IR-prestretch P_{open} differences coupled with microenvironment-dependent channel mechanics during stress could render the same MS cation channel SA in healthy cells but SI in dystrophic cells.

K_{ACh} channels are another SA-SI example. One laboratory reported these Kir channels as SA (Pleumsamran and Kim, 1995), and another (using recombinant channels) reported them as SI (Ji et al., 1998). As for muscle MS cation channels and *Shaker*-IR, this discrepancy might be resolved by reference to the different prestretch P_{open} prevailing in the two situations. Where they were described as SI channels, the Kir channels were first activated almost maximally (via acetylcholine stimulation of G-proteins), then subjected to stretch. By contrast, the SA version of Kir was at relatively low P_{open} before stretch was applied.

Mechanosusceptibility and its partner mechanoprotection

An organized membrane skeleton may contribute to mechanoprotection of *Shaker* in nerve and muscle. Like TREK and NMDA channels (Wan et al., 1999; Paoletti and Ascher, 1994) which are most mechanosusceptible after the cortical cytoskeleton deteriorates, voltage-gated channels in squid axon show evidence of feeling tension when the membrane skeleton is destroyed. Using electron microscopy and electrophysiology plus chaotropic solutions on squid axon, Terakawa and Nakayama (1985) demonstrated that submembranous cytoskeleton dissolves with KCl and KBr, but maintains its integrity with nonchaotropic KF. Inflation of KF-perfused axons has little impact on the action potential or on voltage clamp currents, whereas inflation of KCl- or KBr-perfused axons reversibly depolarizes them and alters their Na^+ and K^+ channel currents. *Shaker*-like channels target preferentially to stiff bilayer microdomains (Martens et al., 2000) which, for the channels they harbor, may be mechanoprotective.

Mechano*in*susceptibility for mechanotransducers?

Shaker-IR showed that it lacks "unshakeable" intrinsic mechanoprotection. For exquisitely sensitive mechanotransducer channels, e.g., hair cell channels (Hudspeth, 1997), what then seems reasonable? Hypermechanosusceptibility? Surely not. Hair cell channels would be better-off inured to bilayer tension fluctuations (unlike *Shaker*-IR), attentive exclusively to mechanical signals along the tiplink axis. Accordingly, they may be extremely stiff and/or may avoid Δ-area conformations. Expressed heterologously (see Garcia-Anoveros et al., 1998), mechanotransducer channels with these characteristics should "fail" as MS channels.

CONCLUSION

We showed that a molecularly altered voltage-gated channel, *Shaker*-IR, is an MS channel. Indirectly, this has

physiological consequences, as it signifies a need for mechanoprotection. Strip away the overlay of in situ mechanoprotection, and "primitive" mechanosusceptibility emerges. Structure-function studies directed at *Shaker*-IR's voltage-dependence may inadvertently uncover explanations (e.g., in-plane area changes) for its mechanosusceptibility.

REFERENCES

Batiza, A. F., I. Rayment, and C. Kung. 1999. Channel gate! Tension, leak and disclosure. *Structure Fold. Des.* 7:R99–R103.

Bezanilla, F. 2000. The voltage sensor in voltage-dependent ion channels. *Physiol. Rev.* 80:555–592.

Conti, F., I. Inoue, F. Kukita, and W. Stuhmer. 1984. Pressure dependence of sodium gating currents in the squid giant axon. *Eur. Biophys. J.* 11:137–147.

Elinder, F., and P. Århem. 1994. Effects of gadolinium on ion channels in the myelinated axon of *Xenopus laevis*: four sites of action. *Biophys. J.* 67:71–83.

Franco-Obregon, Jr., A., and J. B. Lansman. 1994. Mechanosensitive ion channels in skeletal muscle from normal and dystrophic mice. *J. Physiol.* 481:299–309.

Garcia-Anoveros, J., J. A. Garcia, J. D. Liu, and D. P. Corey. 1998. The nematode degenerin UNC-105 forms on channels that are activated by degeneration- or hypercontraction-causing mutations. *Neuron.* 20:1231–1241.

Gu, X. C., P. F. Juranka, and C. E. Morris. 1997. Tethering a voltage-gated channel to the membrane skeleton: a model for studying the impact of mechanical inputs on gating. *Biophys. J.* 72:143a. (Abstract).

Guharay, F., and F. Sachs. 1984. Stretch-activated single ion channel currents in tissue-cultured embryonic chick skeletal muscle. *J. Physiol.* 352:685–701.

Gustin, M. C., X. L. Zhou, B. Martinac, and C. Kung. 1988. A mechanosensitive ion channel in the yeast plasma membrane. *Science.* 242:762–765.

Hamill, O. P., and D. W. McBride, Jr. 1997. Induced membrane hypo/hyper-mechanosensitivity: a limitation of patch-clamp recording. *Annu. Rev. Physiol.* 59:621–631.

Hoshi, T., W. N. Zagotta, and R. W. Aldrich. 1991. Two types of inactivation in *Shaker* K+ channels: effects of alterations in the carboxy-terminal region. *Neuron.* 7:547–556.

Hoshi, T., W. N. Zagotta, and R. W. Aldrich. 1994. *Shaker* potassium channel gating. I. Transitions near the open state. *J. Gen. Physiol.* 103:249–278.

Hudspeth, A. J. 1997. How hearing happens. *Neuron.* 19:947–950.

Ismailov, I. I., B. K. Berdiev, V. G. Shlyonsky, and D. J. Benos. 1997. Mechanosensitivity of an epithelial Na$^+$ channel in planar lipid bilayers: release from Ca^{2+} block. *Biophys. J.* 72:1182–1192.

Ji, S., S. A. John, Y. Lu, and J. N. Weiss. 1998. Mechanosensitivity of the cardiac muscarinic potassium channel. A novel propertied conferred by Kir 3.4 subunit. *J. Biol. Chem.* 273:1324–1328.

Langton, P. D. 1993. Calcium channel currents recorded from isolated myocytes of rat basilar artery are stretch sensitive. *J. Physiol.* 471:1–11.

Lee, C. J., S. Kwon, Y. H. Lee, D. S. Ahn, and B. S. Kang. 2000. Membrane stretch increases the activity of Ca(2+)-activated K+ channels in rabbit coronary vascular smooth muscles. *Yonsei Med. J.* 41:266–272.

Loots, E., and E. Y. Isacoff. 2000. Molecular coupling of S4 to a K(+) channel's slow inactivation gate. *J. Gen. Physiol.* 116:623–636.

Martens, J. R., R. Navarro-Polanco, E. A. Coppock, A. Nishiyama, L. Parshley, T. D. Grobaski, and M. M. Tamkun. 2000. Differential targeting of *Shaker*-like potassium channels to lipid rafts. *J. Biol. Chem.* 275:7443–7446.

Meyer, R., and S. H. Heinemann. 1997. Temperature and pressure dependence of *Shaker* K+ channel N- and C-type inactivation. *Eur. Biophys. J.* 26:433–445.

Morris, C. E. 1992. Are stretch-sensitive channels in molluscan cells and elsewhere physiological mechanotransducers? *Experientia.* 48:852–858.

Morris, C. E. 2000. Mechanosensitive ion channels in eukaryotic cells. *In* Cell Physiology Source Book 3rd Ed. N. Sperelakis, editor. Academic Press, New York. In press.

Morris, C. E., and U. Homann. 2001. Cell surface area regulation and membrane tension. *J. Membr. Biol.* 179:79–102.

Morris, C. E., and R. Horn. 1991. Failure to elicit neuronal macroscopic mechanosensitive currents anticipated by single-channel studies. *Science.* 251:1246–1249.

Morris, C. E., and W. J. Sigurdson. 1989. Stretch-inactivated ion channels coexist with stretch-activated ion channels in neuronal membranes. *Science.* 243:807–809.

Paoletti, P., and P. Ascher. 1994. Mechanosensitivity of NMDA receptors in cultured mouse central neurons. *Neuron.* 13:645–655.

Patel, A. J., E. Honore, F. Maingret, F. Lesage, M. Fink, F. Duprat, and M. Lazdunski. 1998. A mammalian two-pore domain mechano-gated S-like K$^+$ channel. *EMBO J.* 17:4283–4290.

Perozo, E., D. M. Cortes, and L. G. Cuello. 1998. Three-dimensional architecture and gating mechanism of a K+ channel studied by EPR spectroscopy. *Nat. Struct. Biol.* 5:459–469.

Pleumsamran, A., and D. Kim. 1995. Membrane stretch augments the cardiac muscarinic K+ channel activity. *J. Membr. Biol.* 148:287–297.

Sachs, F., and C. E. Morris. 1998. Mechanosensitive ion channels in non-specialized cells. *Rev. Physiol. Biochem. Pharmacol.* 132:1–78.

Sachs, F., C. E. Morris, and O. Hamill. 2000. Does a stretch-inactivated cation channel integrate osmotic and peptidergic signals? *Nat. Neurosci.* 3:847–848.

Sigurdson, W. J., C. E. Morris, B. L. Brezden, and D. R. Gardner. 1987. Stretch-activation of a K$^+$ channel in molluscan heart cells. *J. Exp. Biol.* 127:191–209.

Small, D. L., and C. E. Morris. 1994. Delayed activation of single mechanosensitive channels in *Lymnaea* neurons. *Am. J. Physiol. Cell Physiol.* 267:C598–C606.

Small, D. L., and C. E. Morris. 1995. Pharmacology of stretch-activated K$^+$ channels in *Lymnaea* neurones. *Br. J. Pharmacol.* 114:180–186.

Steffensen, I., W. R. Bates, and C. E. Morris. 1991. Embryogenesis in the presence of blockers of mechanosensitive ion channels. *Dev. Growth Diff.* 33:437–442.

Sukharev, S., M. Betanzos, C.-S. Chiang, and H. R. Guy. 2001. The gating mechanism of the large mechanosensitive channel MscL. *Nature.* 409:720–724.

Tabarean, I. V., P. F. Juranka, and C. E. Morris. 1999. Membrane stretch affects gating modes of a skeletal muscle sodium channel. *Biophys. J.* 77:758–774.

Tabarean, I. V., P. F. Juranka, and C. E. Morris. 2000. Effects of membrane tension on S3–S4 linker deletion variants of *Shaker*-IR. *Biophys. J.* 78:93a. (Abstract).

Terakawa, S., and T. Nakayama. 1985. Are axoplasmic microtubules necessary for membrane excitation? *J. Membr. Biol.* 85:65–77.

Tytgat, J., and P. Daenens. 1997. Effect of lanthanum on voltage-dependent gating of a cloned mammalian neuronal potassium channel. *Brain Res.* 749:232–237.

Vandorpe, D. H., D. Small, A. Dabrowski, and C. E. Morris. 1994. FMRFamide and membrane stretch as activators of the *Aplysia* S-channel. *Biophys. J.* 66:46–58.

Wan, X., P. F. Juranka, and C. E. Morris. 1999. Activation of mechanosensitive currents in traumatized membrane. *Am. J. Physiol. Cell Physiol.* 276:C318–C327.

Wilkinson, N. C., F. Gao, and O. P. Hamill. 1998. Effects of mechano-gated cation channel blockers on *Xenopus* oocyte growth and development. *J. Membr. Biol.* 165:161–174.

Yang, X. C., and F. Sachs . 1989. Block of stretch-activated ion channels in *Xenopus* oocytes by gadolinium and calcium ions. *Science.* 243: 1068–1071.

Yao, W. D., and C. F. Wu. 1999. Auxiliary hyperkinetic beta subunit of K+ channels: regulation of firing properties and K+ currents in *Drosophila* neurons. *J. Neurophysiol.* 81:2472–2484.

Zaccai, G. 2000. How soft is a protein? A protein dynamics force constant measured by neutron scattering. *Science.* 288:1604–1607.

Zhang, Y., and O. P. Hamill. 2000. On the discrepancy between whole-cell and membrane patch mechanosensitivity in *Xenopus* oocytes. *J. Physiol.* 523:101–115.